A patch antenna design for a phased-array applicator for hyperthermia treatment of head and neck tumours

M.M. Paulides*, J.F. Bakker* and G.C. Van Rhoon*

* Erasmus MC - Daniel den Hoed Cancer Center, Department of Radiation Oncology, Rotterdam, The Netherlands

m.paulides@erasmusmc.nl

Abstract: In this study the aim was to design the best antenna for a novel head and neck hyperthermia applicator. Hereto, we firstly investigated the dependence of the SAR pattern as a function of the operating frequency in an example patient anatomy. We found that 433 MHz provides the optimum between penetration depth and power focussing abilities in the head and neck region. Secondly we selected the patch antenna as most promising candidate and changed its design to meet the desired requirements for operation in a water environment. Subsequently, the dimensions of the antenna were optimized for 433 MHz using electromagnetic modelling tools. The electrical properties of the optimized design were analysed by 3D electromagnetic modelling. We conclude that the design provides good reflection characteristics and the desired electrical field pattern. Future research will establish the sensitivity of the design to interior (length, width, feed point, permittivity of the substrate) and exterior parameters (patient, other antennas) and reveal its performance in a circular array.

Introduction

Patients with advanced carcinomas in the head and neck (H&N) region have a dismal prognosis and loco-regional control for this site still poses a major therapeutic challenge. Combining radiotherapy (RT) with simultaneous chemotherapy improves the treatment outcome but at the cost of increased toxicity. Triggered by the phase III trial of Valdagni *et al*. [1] [2], we started the exploration of hyperthermia (HT) applied to the H&N region. Valdagni demonstrated that with a non-specific HT-applicator already a significant increase in local control (from 24% for RT alone versus 69% for RT plus HT) is achieved for metastatic lymphnodes in Stage IV carcinoma of the H&N. However, for an optimal HT treatment of the primary tumour and metastatic lymphnodes a specific H&N HT applicator is warranted. In our opinion such a site specific designed, multi-element, applicator would also enable a substantial improved control of the specific absorption rate (SAR) deposition pattern and is expected to result in a higher quality of the HT-treatment (Wust *et al*.[3]).

For the development of this applicator we first assessed the optimal operating frequency. Hereto we theoretically investigated the dependence of the SAR in the neck as a function of the operating frequency. This is carried out by the calculation of 3D power absorption (PA) distributions in a realistic patient model. An important criterion for the frequency selection is our demand that the applicator must have the flexibility to heat both advanced laterally located tumours and tumours located at the midline of the H&N region. Hence, the PA distribution must be controlled in both the axial and radial direction for which amplitude and phase steering is essential. The ability to obtain a high PA at the center of the neck will be the most challenging and difficult problem to solve because penetration depth is strongly frequency dependent. Therefore we have focussed on investigating the dependence of the PA at the center of the neck as a function of the operating frequency.

After the selection of the optimal frequency, we selected an electromagnetic (EM) antenna for use in a circumferential array and theoretically assessed its performance. The problems involved with hyperthermia antenna design are very different from the design of antennas in free space and are very challenging. Firstly, the antenna normally radiates into a lossy medium (the waterbolus), which has a considerable influence on the impedance, bandwidth and antenna losses [4]. Secondly, the presence of a patient in the near field has a large impact on the reflection characteristics. Thirdly, in contrast to designs for e.g. communications and radar purposes, the aim is to obtain the desired near-field characteristics of the antenna: a dominant polarisation of the electric (E) field in the direction of the patient-axis (head-feet). The polarisation is of importance for obtaining constructive interference of multiple elements within the patient. Fourthly and finally, the antenna behaviour should be stable for powers up to 150 W, where heating of the water environment results in a shift in di-electric properties, i.e. the resonance frequency of the antenna can be affected. In this research we explored the possibilities and pitfalls of a patch antenna for use in the circumferential antenna array for a head and neck hyperthermia applicator.

Materials and Methods

Operating frequency

To assess the optimal frequency for focussed heating in the neck area we exploited a setup of eight dipole anten-

ISSN: 1727-1983

nas surrounding the patient neck. The patient anatomy was created from 69 CT slices obtained at a distance of 2.5 mm from each other. First the anatomy is segmented in tissues (Figure 1) and subsequent the tissue type (di-electric properties [5]) is assigned to each mesh element. For the electromagnetic calculations we used an implementation[1] of the Finite Difference Time Domain (FDTD) method [6] that uses an homogeneous grid. The FDTD method directly implements Maxwell's equations, which are discretized for application at discrete time steps and at discrete positions in space. An infinite de-mineralized water environment[2] was used to model the waterbolus that is normally used to enable an efficient power transfer from the antenna into the patient. The length of the dipole antennas was smaller or equal to half a wavelength in water ($\lambda_{water}/2$) because this changes the efficiency but not the radiation pattern, i.e. 3.75 cm was used for low frequencies ($\leq$ 433 MHz) and 1.75 cm for high frequencies ($>$ 433 MHz). Amplitudes and phases where equal for all antennas to obtain a central focus. The computational domain (waterbolus edges) was truncated by applying Mur's second order Absorbing Boundary Conditions (ABC) [6] to simulate an infinite water domain.

Because our aim was to assess the ability of a set-up to direct power to the central target region, we selected the average power absorption ratio to quantify the relative amount of energy that is absorbed in the target region:

$$average\ PA\ ratio = \frac{\overline{PA}_{target}}{\overline{PA}_{neck}}, \qquad (1)$$

where $\overline{PA}_{target}$ is the average absorption in the target volume (W/m^3) and $\overline{PA}_{neck}$ is the average absorption in the neck volume (W/m^3). This ratio is found to depend little on the size of the neck volume but to a large amount on the dimensions of the target volume [7]. The neck volume is defined as the tissue voxels within a 12 cm x 12 cm x 10 cm brick volume and the target volume was 5 cm x 5 cm x 5 cm as visualized in Figure 1. These dimensions of the target volume where chosen to obtain a sufficient overlap of clinically advanced tumours that are larger than 4 cm in the largest dimension.

Antenna selection

Some key requirements were defined as a start of the antenna selection process. Because the antenna will be embedded in a movable applicator system the antenna should be light weight and small in size. From our experiences with existing HT treatments of deep located tumours we anticipate that for the H&N treatment we will exceed a treatment time of one hour. Since 150 W is the maximum power of the clinically available amplifiers, the antenna should be able to operate at this level

[1]FDTD program developed at TNO-FEL, The Hague, The Netherlands.

[2]Di-electric properties of de-mineralized water are from [8]: 0g/l, 25°C

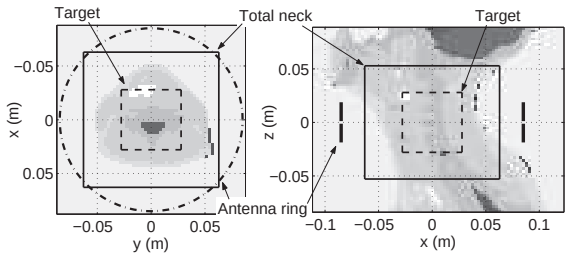

Figure 1: Tissue distribution in the neck of the example patient and positioning of the antennas around the neck. Cross-sections through z = 0 mm (left) and (b) y = 14 mm (right) are visualized.

during treatment time. A high $E_{///}/E_{\perp}$ ratio at the patient skin is desired because E-field components perpendicular to the patient skin lead to high power absorption values at muscle-fat transitions [9]. Furthermore, constructive interference will be optimal for axial electric field components [10]. The antennas will be positioned as close as possible to the patient skin to reduce power losses in the water bolus ($\sigma_{water} \neq 0$ [8]). Therefore, the influence of the patient on the reflection characteristics should be low. A low sensitivity of the reflection coefficient to surrounding influences is normally indicated by a high bandwidth. Further a matched and efficient antenna design is desired to avoid additional power losses in the matching circuit. Little cross-coupling is aimed for because cross-coupling interferes with the independent power and phase steering possibilities of each antenna [11] and thus degrades the steering possibilities of the antenna array.

Antenna design

Deep hyperthermia (DHT) applicators generally consist of an array of dipole or waveguide antennas. Dipole antennas are relatively insensitive to patient loadings but require a matching network containing a balun. Waveguide antennas are rigid and require no matching, however they have a small bandwidth. We selected the patch antenna because they are small and lightweight and can be fed with a simple coaxial cable, where no special matching network is required between antenna and transmission line. Further, a minimal patient-antenna distance can be assured thus the influence of tissue loadings is restricted. In the antenna design proposed here (Figure 3), efficient radiation into the waterbolus is obtained by using water as substrate material, i.e. the patch is submerged in the water. Cross-coupling is expected to be low because due to the absence of a di-electric transition that leads to surface waves. The water will be circulated 1) to cool the patient skin and 2) to cool the patch eliminating self-heating effects at high power.

To speed up the design process we optimized the properties of the design by utilizing the gradient optimizer of a layered-2D EM simulation program (Ansoft Designer) and subsequently a 3D EM simulation program (SEMCAD).

ISSN: 1727-1983

EM model implementations

Ansoft Designer [12] is a layered 2D method of moment (MoM) based program. The program allows to define PEC layers and dielectric layers and subsequent addition of non-infinite PEC (Perfect Electrical Conducting) structures (Figure 2). A constrained gradient optimization algorithm was used to optimize the length (L), width (W) and position of the feed x_f for different heights (h). Layer1 and Layer2 where water and Layer3 was muscle. Layer3 was positioned 10 or 5 cm from the patch, i.e. the thickness of Layer2 was 10 or 5 cm.

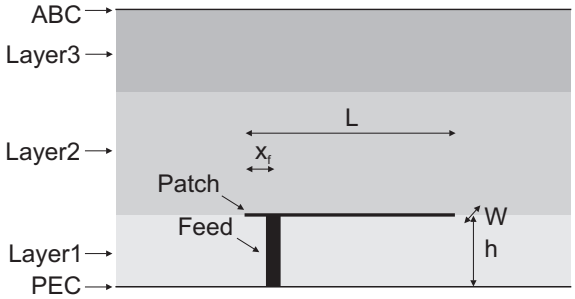

Figure 2: Schematic visualization of the layered patch setup implementation in Designer. "Patch", "Feed" and the groundplane are PEC.

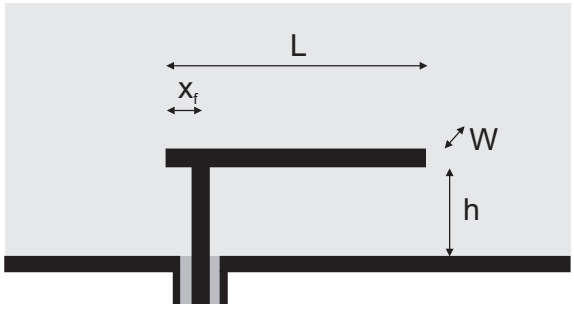

Figure 3: Schematic visualization of the patch design implementation in SEMCAD. PEC structures are in black and water is in light grey.

The implementation of the patch setup in SEMCAD [13] is visualized in Figure 3. We used SEMCAD modelling to refine and analyse the antenna design. SEMCAD is a commercial FDTD [6] algorithm. For the FDTD algorithm, the entire computational domain must be divided in voxels, i.e. small brick shaped elements. SEMCAD supports a variable grid stepping thus refinements at small structures can be used to increase the accuracy of the model while computational time remains acceptable. Four or eight layers of Berenger's Perfect Matched Layers (PML) [6] were used as ABC, where eight layers PML were utilized only at the truncation of the coaxial cable to ensure that all energy was absorbed. We modelled the setup with grid steps from 5 mm down to 0.25 mm. This refinement was necessary because the model appeared quite sensitive to the actual connection point of the central coax conductor to the patch. Further, accurate modelling of the coaxial cable (RG213 /U 50Ω) required a maximum gridstep of 0.3 mm. Four voltage sources were positioned in the coax: 40 mm beneath the ground plane. These sources were excited with a Gaussian pulse containing frequencies between 300 and 600 MHz. The resulting E-field pattern in the coax was investigated to ensure that the correct mode was propagating towards the patch. Voltages and currents were recorded at the location of the groundplane so the S-parameters could be calculated. Simulations were terminated when signals where sufficiently small ($<0.01\%$).

Results

The SAR distribution at 433 MHz for the example patient is visualized in Figure 4. Clearly a central focus is visible in both the sagittal and transversal plane. Further, high absorption values can be seen in the transversal plane at the skin. It is expected that this superficial absorption can be effectively cooled by circulating water bolus water.

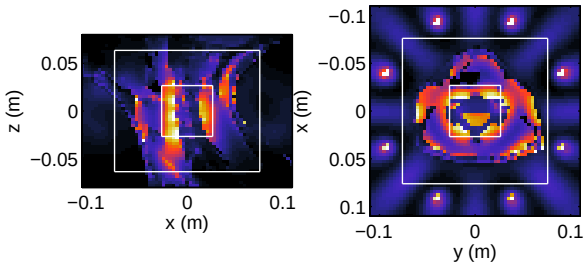

Figure 4: Cross-sections though z = 0 mm (left) and y = 14 mm (right) of the SAR distribution in the example patient. The colorscale is from black ($PA = 0$) to white ($PA = 5 \cdot \overline{PA}_{neck}$).

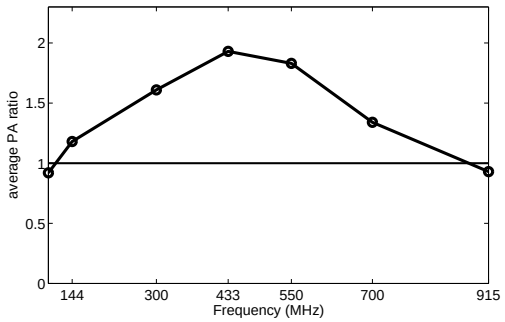

Figure 5: Average PA ratio values calculated with FDTD as a function of frequency for different target volume sizes. Average PA ratio = 1, i.e. the average PA in target and neck volume are equal, is indicated. The target volume was 5 cm x 5 cm x 5 cm and the neck volume was 12 cm x 12 cm x 10 cm

Figure 5 shows the average PA ratio as a function of frequency for the example anatomy. The target volume is

ISSN: 1727-1983

located centrally thus the possibility to direct the energy to the central region is investigated. These results show that 433 MHz is a suitable choice for directing the energy efficiently into the target region. At this frequency the average PA in the target region is two-fold the average PA in the neck.

Patch antenna

In contrast to our expectations it was found that a resonant antenna was obtained only at heights (h = substrate thickness) larger than 5 mm and lengths much smaller than $\lambda_{water}/2$. Table 1 shows the optimized dimensions of the patch antenna for substrate thicknesses larger than 5 mm. Clearly an optimum h for the setup can be observed at 8 mm. However, all values are well beneath -20 dB: thus acceptable. Further it can be noted that the optimal length L_{opt} decreases a little for an increased height whereas W_{opt} is much more unstable. The influence of the presence of a muscle layer (Figure 2 : Layer3) at a minimum distance of 5 cm was found to be low.

Table 1: Optimized dimensions and corresponding reflection coefficient at 433 MHz for various substrate thicknesses (h) as found using the gradient optimizer of Ansoft Designer.

h	L_{opt}	W_{opt}	$x_{f,opt}$	S_{11} (433 MHz)
5	31.8	15.6	0.0	-26 dB
7	30.2	10.6	2.5	-30 dB
8	28.3	12.5	0.3	-34 dB
9	27.8	10.0	1.5	-29 dB
10	27.4	15.1	2.9	-25 dB

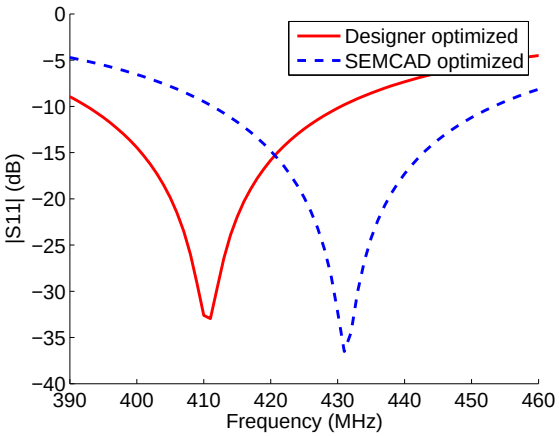

Figure 6: Reflection coefficient calculated from the results of FDTD for the Designer optimized and SEMCAD optimized setup.

The reflection characteristics predicted by SEMCAD of the optimal Ansoft optimized setup for h = 8 mm, i.e. L = 28.3 mm, W = 12.5 mm and x_f = 0.3 mm, is visualized in Figure 6. Using SEMCAD, the length (L) of this setup was scaled to find a resonant antenna at 433 MHz, i.e. the length of the SEMCAD optimized setup was 26.4 mm (Figure 6). This figure shows that a consistent shift of 22 MHz in resonance frequency is predicted by the FDTD program compared to the results of Designer. The bandwidth predicted by SEMCAD (∼5%) is found to be lower than the bandwidth of Designer (∼7%). This -15dB bandwidth is quite high compared to a "normal" patch: approximately 5% (21 MHz) for all setups, where generally 1% is obtained [14]. This high bandwidth is essential since it indicates a low sensitivity of the reflection coefficient to patient loadings.

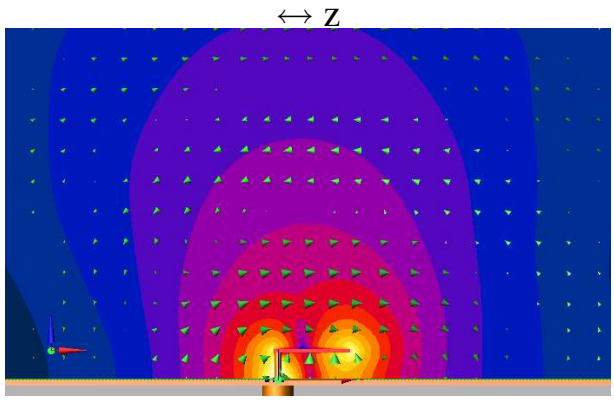

Figure 7: Solid model of the patch antenna and its corresponding RMS value (dB) of the E-field (black = -50 dB and white = 0 dB). The value and orientation of the instantaneous E-field is indicated by the arrows.

Figure 7 shows the E-field predicted by FDTD of the patch implementation. It shows both the amplitude and direction of the field. The field pattern is very similar to that of a dipole antenna thus the approximation by dipoles to find the optimal frequency is therefore justified. The prediction indicates that a large part of the electric field is propagating "upwards", i.e. towards the patient. Further, a dominant field in the z-direction is predicted at distances greater than 4 cm ($\sim \lambda_{water}/2$) from the patch antenna, which is an essential requirement for constructive interference as explained in the introduction.

Conclusions

The most suitable operating frequency for hyperthermia treatment of H&N tumours, i.e. 433 MHz, is selected based on EM simulations with an example patient. At this frequency a good central SAR focus is obtained. Subsequently, a patch antenna has been designed for operation at this frequency. We conclude that the design is feasible and meets with the requirements for the head and neck applicator that are investigated, i.e. the simulations predict a high bandwidth (>5%) a good $E_{//}/E_{\perp}$ ratio and little influence of the presence of a patient (muscle layer).

In future steps we will establish the sensitivity of the

ISSN: 1727-1983

design to both internal influences (length, width, height, permittivity of the water) and external influences (patient, cross-coupling with neighbouring patch antennas) by simulations and measurements. Further, the SAR pattern, and steering possibilities, that can be obtained by a circumferential array of multiple of these patch antenna elements will be investigated.

Acknowledgements

This work is financially supported by the Dutch Cancer Society, grant DDHK 2003-2855. The authors further would like to thank J.H.M. Strijbos, T. Bertuch and P. Futter for their various contributions.

References

[1] Valdagni R., Liu F-F. and Kapp S. (1988): 'Important prognostic factors influencing outcome of combined radiation and hyperthermia', *Int. J. Radiat. Oncol. Biol. Phys.*, **15**, pp. 959-972

[2] Valdagni R. and Amichetti M. (1993): 'Report of long-term follow-up in a randomized trial comparing radiation therapy and radiation therapy plus hyperthermia to metastatic lymphnodes in stage IV head and neck patients', *Int. J. Radiat. Oncol. Biol. Phys.*, **28**, pp. 163-169.

[3] Wust P., Seebas M., Nadobny J., Deuflhard P., Mónich G., Felix R. (1996): 'Simulation studies promote technological development of radiofrequency phased array hyperthermia', *Int. J. Hyperthermia*, **12**, pp. 477-498.

[4] Hand J.W., James J.R. (1986): 'Physical Techniques in Clinical Hyperthermia', Research Studies Press LTD. 58B Station Road, Letchworth, Herts, SG6 3BE, England, ISBN: 0-86380-037-8, Chapter 4

[5] Gabriel S., Lau R.W. and Gabriel C. (1996): 'The dielectric properties of biological tissues III: Parametric models for the dielectric spectrum of tissues', *Phys. Med. Biol.*, **41**, pp. 2271-2293

[6] Taflove A. (1995): 'Computational electrodynamics: The Finite-Difference Time-Domain Method', Artech House, 685 Canton Street, Norwood, MA 02062. ISBN: 0-89006-792-9, Chapter 3 & 6

[7] Paulides M.M., Vossen S.H.J.A., Zwamborn A.P.M. and Van Rhoon G.C. 'Theoretical investigation into the feasibility to deposit RF energy centrally in the head and neck region', *Int. Rad. Onc. Biol. Phys.*, *In press*.

[8] Stogryn A. (1971): 'Equations for Calculating the Dielectric Constant of Saline Water (Correspondence)', *IEEE Trans. Micr. Theor. Tech.*, **19**, pp. 733-736

[9] Paulides M.M., Wielheesen D.H.M., Van der Zee J. and Van Rhoon G.C. (2005): 'Assessment of the local SAR distortion by major anatomical structures in a cylindrical neck phantom', *Int. J. Hyperthermia*, **21**, pp. 125-140

[10] Field S.B. and Franconi C. (1987): 'Physics and Technology of Hyperthermia', Martinus Nijhoff Publishers, P.O. box 163, 330 AD Dordrecht. ISBN: 90-247-3509-2, Chapter I-7

[11] Wust P., Seebas M., Gellerman J., Deuflhard P., Nadobny J. (2001): 'Antenna arrays in the SIGMA-eye applicator: Interactions and tranforming networks', *Med. Phys.*, **28**, pp. 1793-1805

[12] Ansoft Designer, Ansoft Coorporation, Internet site address: http://www.ansoft.com

[13] SEMCAD: the Simulation platform for EMC, Antenna Design and Dosimetry, Smith and Partner Engineering AG, Internet site address: http://www.semcad.com

[14] Garg R., Bhartia P., Bahl I., Ittipiboon A. (2001): 'Microstrip antenna design handbook', Artech House, 685 Canton Street, Norwood, MA 02062. ISBN: 0-89006-513-6.

ISSN: 1727-1983